

# Ignition by laser radiation and combustion of composite solid propellants with bimetal powders

A G Korotkikh<sup>1,2</sup>, V A Arkhipov<sup>2</sup>, O G Glotov<sup>3</sup> and N N Zolotarev<sup>2</sup>

<sup>1</sup>Institute of Power Engineering, Tomsk Polytechnic University, 634050, Tomsk, 30 Lenin Ave., Russia

<sup>2</sup>Research Institute of Applied Mathematics and Mechanics, Tomsk State University, 634050, Tomsk, 36 Lenin Ave., Russia

<sup>3</sup>Institute of Chemical Kinetics and Combustion of SB RAS, 630090, Novosibirsk, 3 Institutskaya Str., Russia

E-mail: korotkikh@tpu.ru

**Abstract.** The use of metal powder (usually aluminum) as a fuel in composite solid propellants (CSPs) for propulsion is the most energy efficient method that allows improvement of combustion characteristics of propellants in the combustion chamber and specific impulse. This paper presents the experimental data of the ignition and combustion processes of CSPs containing Alex aluminum nanopowder and mixtures of Alex/Fe and Alex/B nanopowders. It was found that the introduction of Alex/Fe in CSPs leads to 1.3–1.9 times decrease in the ignition time at  $q = 55\text{--}220\text{ W/cm}^2$  and to 1.3–1.4 times increase in the burning rate at  $p = 2.2\text{--}7.5\text{ MPa}$  with respect to that for basic CSP with Alex. When introducing Alex/B in CSP, the ignition times are 1.2–1.4 fold decreased, and the burning rate is practically unchanged. However, the agglomeration is significantly enhanced, which is manifested through the increase in the agglomerate particles content in condensed combustion products by a factor of 1.8–2.2, at 1.6–1.7 fold increase of the agglomerates mean diameter for CSP with Alex/B.

## 1. Introduction

Modern composite solid propellants (CSPs) contain the oxidizer crystals of ammonium perchlorate (AP), ammonium nitrate (AN) and nitramines (RDX, HMX, CL-20) [1–2], combustible-binder – inert or energetic polymer rubber, and metal fuel – aluminum powder with typical content up to 22 wt.% [3–5]. These systems are used as the energy source of solid rocket motors and gas generators for various purposes. Adjustment of the CSP burning rate is mainly achieved by introduction of the catalysts in propellant formulation, through partial or complete replacement of AP and AN by nitramines, by changes of the excess oxidizer factor, as well as the changed particle size of oxidizer and metal powders.

Metal oxides:  $\text{MnO}_2$ ,  $\text{Ni}_2\text{O}_3$ ,  $\text{Cr}_2\text{O}_3$ ,  $\text{MgO}$ ,  $\text{Fe}_2\text{O}_3$ ,  $\text{Co}_2\text{O}_3$ ,  $\text{CuO}$ ,  $\text{SiO}_2$ , copper, iron, zinc, cadmium and magnesium salts of chromic and metachromic acids, complex cyanides of copper, iron and nickel are used as burning catalysts of CSPs [6–9]. The most common and versatile in this group of catalysts are the systems containing copper, chromium, boron and iron [10–12].



This paper presents the experimental data on ignition, combustion and agglomeration processes of CSPs based on Alex aluminum nanopowder (NP) containing additives of iron and amorphous boron.

## 2. Experimental

### 3.1. The CSP samples

We studied the CSP samples on the basis of bidisperse AP (fraction less than 50  $\mu\text{m}$  and 160–315  $\mu\text{m}$  in the ratio 40/60), inert combustible-binder (19.7 wt.%) – butadiene rubber plasticized by transformer oil, and Alex aluminum NP (15.7 wt.%) obtained in argon using electric explosion of conductors. In the second and third compositions of CSPs, 2 wt.% of the Alex NP was partially replaced by 2 wt.% additives of iron and amorphous boron NPs. According to the measurements on the BET analyzer Nova 2200e, the specific surface area of Alex amounts to 7.04  $\text{m}^2/\text{g}$  in nitrogen, 1.08  $\text{m}^2/\text{g}$  in iron, and 8.63  $\text{m}^2/\text{g}$  in amorphous boron. The studied cylindrical samples of CSPs with a diameter of 10 mm and height of 30 mm were produced in the laboratory by extrusion pressing with the subsequent curing. The density of solid samples was in an interval of 1.53–1.59  $\text{g}/\text{cm}^3$  depending on the component composition.

### 3.2. Ignition by laser radiation of CSPs

The ignition study of test CSPs was carried with the use of a set up for radiant heating on the basis of  $\text{CO}_2$ -laser with the wavelength of 10.6  $\mu\text{m}$  and power of 200 W (Figure 1). Prior to testing, the samples were cut into tablets of 5 mm height. The CSP samples were placed in the hollow cylinder of 10 mm depth made of ebonite for inhibiting the lateral surface and making one-dimensional flow of gasification products.

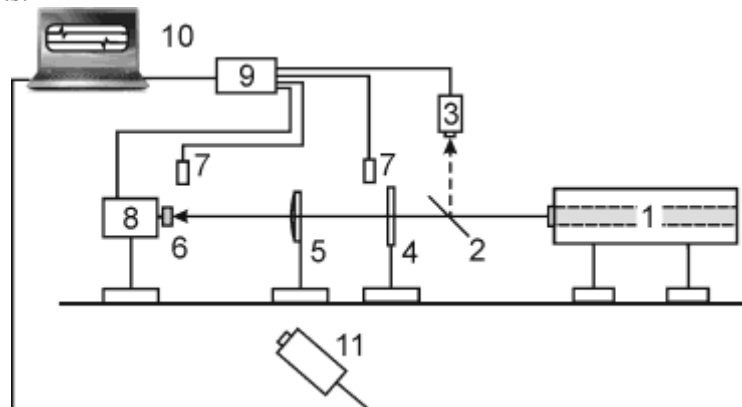


**Figure 1.** The scheme of experimental setup based on  $\text{CO}_2$ -laser:  $\text{CO}_2$ -laser (1); beam-splitting mirror (2); thermoelectric sensor of radiation power (3); shutter (4); lens (5); CSP sample (6); photodiodes (7); transducer of recoil force (8); ADCs (9); PC (10); video camera (11)

Test CSP sample (6) was attached to the substrate of recoil force transducer (8) to record the gasification products outflow from the burning surface. Shutter (4) being opened, radiation was focused onto CSP sample (6) by sodium chloride lens (5). Signals from recoil force transducer (8) and photodiodes (7) were transmitted to L-card-E 14-440 ADC (9) and recorded in personal computer (10), and then processed using LGraph2 software. The time delay of start gasification  $t_{gas}$  of the CSP sample was determined as the time interval between the moments of signals change of photodiode near shutter (7) (or a thermocouple installed in the laser beam behind the shutter), and recoil force transducer (8). Photodiode (7) recorded the moment of opening the shutter, transducer (8) recorded the appearance of recoil force signal of gasification products flowing from the front (irradiated) sample surface. The ignition time  $t_{ign}$  of CSPs was determined by difference between the moments of signals

from two photodiodes (7), one of which recorded the appearance of flame near the end surface of the CSP sample. The relative error of delay times measuring of  $t_{gas}$  and  $t_{ign}$  was equal to 5–12 % at the value of confidence probability 0.9.

The values of recoil force of gasification products outflow from the end surface of the CSP sample during heating of the reaction layer, ignition and combustion of CSPs were determined using a recoil force transducer [13].

The radiation power and heat flux density of CO<sub>2</sub>-laser beam was measured by the thermoelectric sensor of radiation power (3). The maximum radiation power was defined in the center of the laser beam.

### 3.3. Combustion of CSPs

The study of the effect of iron and amorphous boron additives on the combustion process of CSPs was conducted in blow-through sampling bomb in nitrogen at different pressures [14]. We used the CSP samples with a diameter of 10 mm and height of 25–30 mm in the experiments with sampling of condensed combustion products (CCP). The lateral surface of the samples was inhibited by heat resistant rubber "Solpren" (a styrene/butadiene copolymer). During combustion of Solpren, the carbonaceous particles were formed, the content of which in CCPs did not exceed 1 wt.%.

The experiments were carried out in nitrogen at three pressure levels: 2.2, 4.5, and 7.5 MPa. The CSP burning rate was determined on the basis of the known initial length and the burning time of the sample, which was measured via processing the signal from a pressure sensor installed in a bomb. During combustion of the CSP sample, gaseous and condensed combustion products passed through the metal sieve mesh packet and analytical aerosol filter which capture solid particles of different sizes. The sampled particles of combustion products were divided into two fractions: less than 80 μm and 80–315 μm. Then, the CCPs particles were subjected to morphological, particle size, chemical, and phase analyses.

## 3. Results and discussion

### 3.1. Ignition parameters

The values of ignition and gasification times, recoil force of gasification products outflow for the test solid propellants samples under study in atmospheric conditions were determined using a laser setup. Processing of signal recording from the recoil force transducer, the time delays of ignition and gasification, the recoil force outflow of gasification products from the burning surface of CSP samples was performed. The ignition time of CSPs dependences vs. the maximum value of the heat flux density (in the center of the laser beam) were determined (Figure 2).

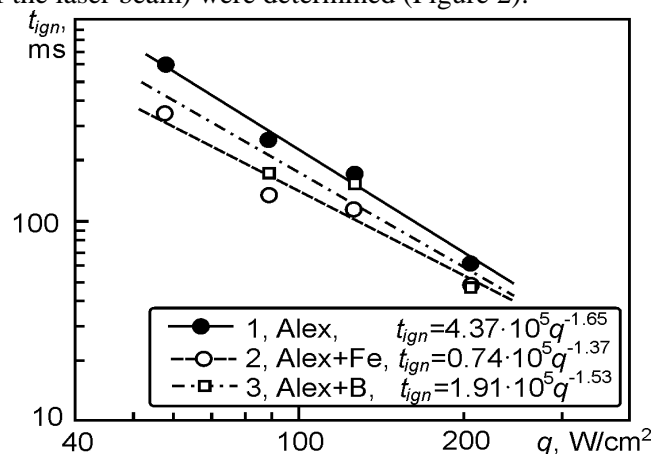


**Figure 2.** The ignition time of CSPs with metals vs. the heat flux density

Partial replacement of Alex by iron in CSP leads to 1.3–1.9 fold decrease in the ignition time in the range of heat flux density 55–220 W/cm<sup>2</sup>. Partial replacement of Alex by boron in CSP leads to 1.2–1.4 fold decrease in the ignition time in the specified range of  $q$ . For the CSP sample with Alex, the gasification starts immediately after shutter opening and the gasification time is 40 times less than the ignition time at the heat radiant flux density of  $q = 65$  W/cm<sup>2</sup>. For samples with Alex/Fe and Alex/B, the time moments of ignition start and gasification start coincide. Partial replacement of Alex by iron in CSP in initiation by CO<sub>2</sub>-laser leads to 25 fold increase of the gasification time and 1.3 fold increase of the recoil force of gasification products outflow from the burning surface in the period of stationary combustion of CSPs. For partial replacement of Alex by boron in the CSP composition, the gasification time increases 36 times and the recoil force of gasification products outflow increases 1.1 times.

Thus, the additives of iron and boron in the CSPs with Alex allow considerable increase in the gasification time and reduction of the ignition time and also increase in the recoil force of gasification products outflow from the burning surface of CSP samples.

### 3.2. Combustion and agglomeration parameters

Figure 3 shows the dependencies of the burning rate on pressure for test CSPs in the form

$$u = B \cdot p^n,$$

where  $[u]$  in mm/s,  $[p]$  in MPa, and also the values of determination coefficient  $R^2$  characterizing the quality of approximation.

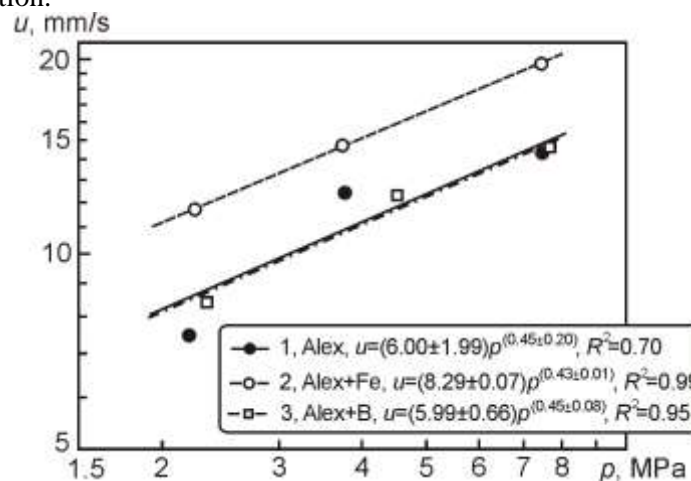


**Figure 3.** The burning rate of CSPs with metals vs. pressure

As one can see, the dependencies of the burning rate on pressure for CSP with Alex and Alex/B are matched up within the range of experimental error. The CSP with Alex/Fe does not change the exponent of the burning rate law, but leads to significant increase in the burning rate level (from 7.5 to 11.7 mm/s at  $p = 2.2$  MPa and from 14.3 to 19.7 mm/s at  $p = 7.5$  MPa).

A noticeable increase in the burning rate of iron doped CSP can be possibly explained by the iron oxide catalytic effect on the oxidizer decomposition and corresponding increase in the heat release on the burning surface of sample. The thermal analysis data obtained with a thermal analyzer Netzsch STA 449 F3 Jupiter at the heating rate of 10 K/min in argon have shown that the CSP temperature of intensive decomposition beginning is reduced by  $\sim 20$  K upon iron addition. Note also that there is a possibility for thermite reaction between fine aluminum particles and iron oxide (total content in CSP formulation amounts to  $\sim 0.16$  wt.%) within the subsurface reaction layer resulting in additional release of heat.

Boron additive in CSP formulation does not make catalytic effect on the propellant decomposition. The thermal analysis data shows that the start temperature of intensive decomposition of CSP with Alex/B remains practically unchanged and amounts to 582 K. Consequently, the burning rate of boron doped CSP exhibits the same behavior as original Alex-based CSP.

Figure 4 shows the values of the mean diameter and dimensional parameters of sampled agglomerate particles of CCPs (with  $D > 55 \mu\text{m}$ ). Within the confidence intervals, the scatter of the experimental data on the CCPs parameters (typical error bars) is the same for all tested CSPs.

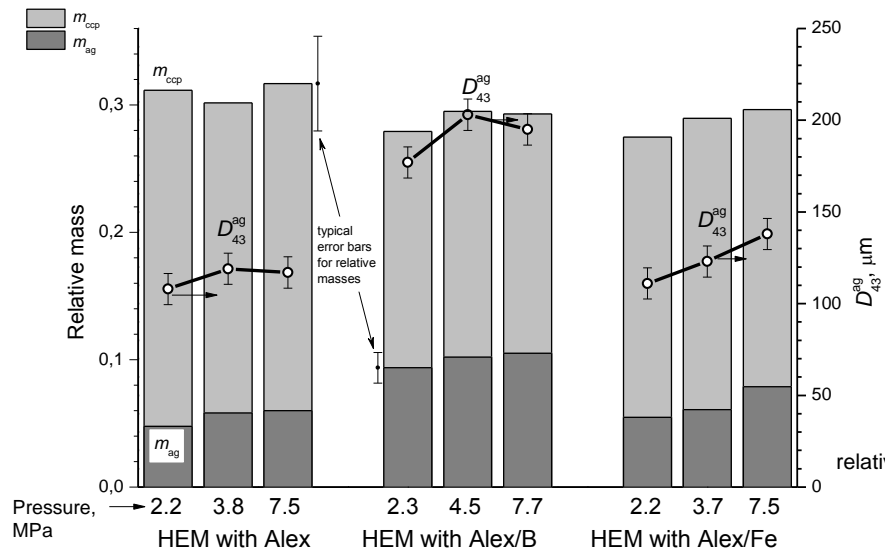


**Figure 4.** Agglomerate mean diameter and values of agglomerate relative mass  $m_{ag}$  and CCPs relative mass  $m_{ccp}$  for CSPs with metals

The relative mass of agglomerates  $m_{ag}$  (blacked bars in Figure 4) is increased with the growth of ambient pressure for all CSPs. In the case of CSPs with Alex and Alex/Fe, the values of the relative mass parameters of agglomerates  $m_{ag}$ , the fraction of metal involved in agglomerate formation and the mean diameter, characterizing the agglomerates properties, are similar. Since the burning rate of CSP with Alex/Fe is higher as compared with CSP with Alex but the agglomerating parameters of CCPs are similar, one can state that agglomeration in the case of CSP with Alex/Fe is conditionally enhanced and this is compensated due to the increase in the burning rate.

For CSP with Alex/B, the relative mass of agglomerates  $m_{ag}$ , the fraction of agglomerates in CCPs  $m_{ag}/m_{ccp}$  and the fraction of metal involved in the formation of agglomerates are increased. In addition, the agglomerates of CSP with Alex/B are much larger in size (the mean diameter is increased). Taking into account the similar levels of the burning rate, as well as the identity of the geometric structure of CSPs (which is mainly determined by the coarse particles of AP), these facts should be definitely interpreted as an agglomeration enhancement upon introduction of boron.

In all cases, the aluminum content in the fraction of  $< 80 \mu\text{m}$  does not exceed 1.3 wt.%. It can be expected that the particles with  $D < 55 \mu\text{m}$  contain a smaller amount of unburned aluminum. The analysis of the mass size distributions of oxide particles showed that in all cases (except for CSP with Alex at  $p = 2.2 \text{ MPa}$ ) the basic modes of size distributions are in the same ranges of the particle size analyzer Malvern. Thus, the first mode is observed in the range of 1.9–2.4  $\mu\text{m}$ , most "massive" mode is in the range of 3–11  $\mu\text{m}$ . In the case of CSP with Alex/B and Alex/Fe, the amplitude of the first mode is much larger than in the case of CSP with Alex. The particles formation of micron and submicron size is normally associated with the vapor type combustion of aluminum. Actually, the mass size distributions of fine particles for the studied CSPs have different ratios of mode amplitudes and they are slightly changed with the pressure. The variation of the ratio of modes results in different

magnitudes of the mean diameters: for CSPs with Alex, Alex/B and Alex/Fe they are about 6.4  $\mu\text{m}$ , 4.8  $\mu\text{m}$  and 5.9  $\mu\text{m}$ , respectively.

#### 4. Conclusions

1. The effect of iron and amorphous boron nanoadditives in CSP on the basis of AP, butadiene rubber and 15.7 wt.% of aluminum Alex on ignition and combustion characteristics were studied. It was found that the introduction of Alex/Fe in CSP decreases the ignition time by a factor of 1.3–1.9 for the range of heat flux density of 55–220  $\text{W}/\text{cm}^2$ , increases the recoil force of gasification products outflow from burning surface by a factor of 1.3 in the period of stationary combustion of propellants due to possible catalytic effect, which reduces the beginning temperature of AP high-temperature decomposition in the reaction layer of CSP by 20  $^{\circ}\text{C}$  and interaction of thermite mixture of aluminum and iron particles in the reaction layer of propellants. At the same time, the burning rate of the CSP sample is increased by a factor of 1.3–1.4 in the pressure range of 2.2–7.5 MPa and the agglomeration of metal fuel is slightly increased: the mean diameter of agglomerate particles is increased up to 1.2 fold and the content of agglomerates in the CCPs composition is increased up to 1.4 fold. The content and mean diameter of oxide particles in CCPs are reduced by 16% and 13%, respectively.

2. The introduction of Alex/B in CSP decreases the ignition time by a factor of 1.2–1.4 at  $q = 55\text{--}220 \text{ W}/\text{cm}^2$  and increases of the recoil force of gasification products outflow from the burning surface by a factor of 1.1. In this, the beginning temperature of CSP high-temperature decomposition does not change and equals to  $\sim 309 \text{ }^{\circ}\text{C}$ . The burning rate is practically unchanged with respect to the CSP sample with Alex. However, the agglomeration is significantly enhanced, which is manifested through 1.8–2.2 fold increase in the agglomerate particles content in CCPs composition, 1.6–1.7 fold increase in the agglomerates mean diameter and 1.6–1.9 fold increase in the metal fraction, which is involved in agglomerates formation. The content and the mean diameter of the oxide particles in CCPs are reduced more significantly than those upon introduction of iron, by a factor of 1.2–1.3 and 1.3–1.4, respectively.

#### Acknowledgement

This work was supported by the Ministry of Education and Science of the Russian Federation under Agreement No. 14.577.21.0157 of 11.28.2014 (unique identifier RFMEFI57714X0157).

#### References

- [1] Beckstead M W, Puduppakkama K, Thakreb P and Yang V 2007 *Progress in Energy and Combustion Science* **33** pp 497–551
- [2] Takahashi K, Oide Sh and Kuwahara T 2013 *Propellants, Explosives, Pyrotechnics* **38** pp 555–562
- [3] Sossi A, Duranti E, Manzoni M, Paravan C, DeLuca L T, Vorozhtsov A B, Lerner M I, Rodkevich N G, Gromov A A and Savin E N 2013 *Combustion Science and Technology* **185** pp 17–36
- [4] Arkhipov V A and Korotkikh A G 2012 *Combustion and Flame* **159** pp 409–415
- [5] Arkhipov V A, Bondarchuk S S, Korotkikh A G, Kuznetsov V T, Gromov A A, Volkov S A and Revyagin L N 2012 *Combustion, Explosion, and Shock Waves* **48** pp 625–635
- [6] Arkhipov V A, Bondarchuk S S and Korotkikh A G 2010 *Combustion, Explosion, and Shock Waves* **46** pp 570–577
- [7] Shioya S, Kohga M and Naya T 2014 *Combustion and Flame* **161** pp 620–630
- [8] Ishitha K and Ramakrishna P A 2014 *Combustion and Flame* **161** pp 2717–2728
- [9] Farley C W, Pantoya M L and Levitas V I 2014 *Combustion and Flame* **161** pp 131–1134
- [10] Berner M K, Talawar M B, Zarko V E 2013 *Combustion, Explosion, and Shock Waves* **49** pp 625–647
- [11] McDonald B A, Rice J R and Kirkham M W 2014 *Combustion and Flame* **161** pp 363–369

- [12] Zarko V E and Glotov O G 2013 *Science and Technology of Energetic Materials* **74** pp 139–143
- [13] Arkhipov V A, Kiskin A B, Zarko V E, Korotkikh A G 2014 *Combustion, Explosion, and Shock Waves* **50** pp 622–624
- [14] Glotov O G, Zyryanov V Ya 1995 *Combustion, Explosion and Shock Waves* **31** pp 72–78